31. GEOCHEMISTRY OF INTERSTITIAL WATERS

31.1. INTERSTITIAL WATER STUDIES ON SMALL CORE SAMPLES FROM THE MEDITERRANEAN SEA[1]

F. L. Sayles and L. S. Waterman, Woods Hole Oceanographic Institution, Woods Hole, Massachusetts
and
F. T. Manheim, U. S. Geological Survey, Woods Hole Oceanographic Institution, Woods Hole, Massachusetts

ABSTRACT

Of ten Leg 13 sites studied by us, eight give definite evidence of the existence of halite-containing sediments beneath the seabed. This conclusion is based on the existence of continuous sodium and chloride enrichments in interstitial waters with depth. This is the only direct evidence of the existence of salt at these sites, for only evaporitic dolomite, gypsum, and/or anhydrite were recovered in cores. Among other ionic relationships, influence of evaporites is seen in calcium, magnesium and sulfate concentrations. Record high barium (216 ppm) and strontium (345 ppm) concentrations were observed in sulfate depleted pore fluids of Site 128 in the Hellenic Trench.

INTRODUCTION

The sediments cored on Leg 13 are, for the most part, characterized by high sedimentation rates and usually contain large proportions of terrigenous detritus. Upper Miocene evaporites are widespread throughout the deep basins, and underlie most of the Leg 13 sites. It is to be expected that the influence of both normal diagenesis and underlying evaporites will be seen in the composition of interstitial solutions.

Previous experience has demonstrated that diffusion of salts from evaporite sequences into overlying sediments may strongly influence the composition of interstitial solutions in the superjacent sediments. Increases in interstitial Na and Cl concentration with depth have been found to be characteristic of sediments overlying known salt deposits in the Gulf of Mexico (Manheim and Bischoff, 1969; Manheim and Sayles, 1969; Manheim *et al.*, 1972). Data from Leg 10 of the Deep Sea Drilling Project in the Gulf of Mexico and Manheim and Bischoff (1969) demonstrate that large Mg concentration increases may occur with the more characteristic Na and Cl enrichments. Increases in Ca and SO_4 concentration may occur at least locally through the dissolution of gypsum and anhydrite.

Concentration changes resulting from diagenetic reactions not related to evaporites are readily distinguishable from those associated with dissolution and diagenesis of evaporites. Normal marine diagenesis produces little or no significant change in Na and Cl concentrations in most cases. In the rare cases where changes are noted, they are depletions. Mg and SO_4 have not been found to be enriched in normal marine sedimentary sequences in previous DSDP studies, but depletions of both are common. Characteristically, the greatest diagenetic changes in pore fluid composition are observed in rapidly deposited sediments (>5 cm/10^3 years) containing appreciable amounts of terrigenous material.

The analytical methods utilized are those previously employed in this laboratory and described in earlier reports. We gratefully acknowledge the assistance of James O'Neill and Joanne Goudreau in the analysis of these samples.

RESULTS

The analytical data are presented in Tables 1 and 2 (major and minor constituents, respectively). The data are subject to uncertainties arising chiefly from two sources: Ca loss due to $CaCO_3$ precipitation, and temperature-of-squeezing effects. In sediments where SO_4 is strongly reduced and alkalinities are increased above 10 meq/kg, Ca and alkalinity loss due to $CaCO_3$ precipitation after squeezing has been noted (Gieskes, 1972). Extensive reduction of SO_4 is common in the Leg 13 samples, but alkalinities have not exceeded 8 meq/kg. Serious Ca and alkalinity losses have not been found in studies of such samples (Gieskes, 1972; Sayles *et al.*, 1972). Small losses, however, cannot be ruled out completely. While we believe the depletions of Ca found are real, the *in situ* depletions may be somewhat smaller than our data indicate, and the alkalinities reported may be low.

A second source of uncertainty arises from the effects of warming sediments from *in situ* to laboratory temperatures prior to squeezing. Such treatment leads to depletions of Ca and Mg, and enrichments of Na and K (Mangelsdorf, *et al.*, 1969). Silica is also enriched upon warming (Fanning and Pilson, 1971). These changes do not obscure the existing major ion trends, and with the exception of K, concentra-

[1] Site 126 was located below the evaporites in a deep cleft in the Mediterranean Ridge which cuts through the inferred evaporite layer.

TABLE 1
Major Constituents of Pore Fluids. Values in g/kg (‰) Except as Noted

Sample Designation	Depth (m)	Age	Description	Na[a]	Na[b]	K	Ca	Mg	Total Cations (meq/kg)	Cl	SO_4	Alk. (meq/kg)	HCO_3[c]	Total Anions (meq/kg)	Sum[d]	Refractometer	H_2O (‰)	pH
Hole 121 (36° 09.65′N, 04° 22.43′W, water depth 1163m, Alboran Basin)																		
Surface ocean water				11.2	10.9	0.40	0.44	1.31	614	20.08	2.81	2.6	0.16	628	36.4	36.3	–	–
121-1-3	65	Quaternary	Dark greenish gray marl ooze, plastic	12.3	11.8	0.35	0.18	0.92	607	21.80	0.26	8.4	0.51	628	36.3	35.8	29	7.6
3-3	160	Quaternary	Dark greenish gray marl ooze, plastic	13.4	13.1	0.31	0.48	1.02	684	24.63	<0.05	5.8	0.35	700	40.2	40.2	30	–
4-4	252	Quaternary	Dark greenish gray marl ooze, plastic	14.9	14.7	0.26	0.76	1.19	780	27.92	<0.05	3.2	0.20	790	45.3	45.6	23	7.6
Hole 122 (40° 26.87′N, 02° 37.46′E, water depth 2146m, Valencia Trough)																		
122-2-2	95	Upper Pliocene	Varicolored brown and gray alternations of fine sands and clays	13.0	12.2	0.34	0.83	1.31	689	22.54	4.05	1.4	0.08	721	42.2	41.8	–	7.5
Hole 123 (40° 37.83′N, 02° 50.27′E, water depth 2290m, Valencia Trough)																		
123-1-3	85	Quaternary	Olive gray clays and sand, turbidites	12.5	12.0	0.35	0.41	1.34	662	22.29	2.48	4.8	0.29	684	39.7	40.2	–	7.9
5-2	219	Lower Pliocene	Varicolored gray and brown nanno to marl ooze, fine layers of silt or fine sand	18.0	17.5	0.31	1.30	1.30	941	32.22	2.57	2.2	0.14	964	55.8	56.6	24	7.4
Hole 124 (38° 52.38′N, 04° 59.69′E, water depth 2726m, Balearic Basin)																		
124-1, CC	128	Pleistocene	Varicolored gray terrigenous nanno ooze, plastic, mottling	21.2	20.5	0.33	0.69	1.44	1051	37.01	1.67	2.1	0.13	1080	62.5	62.2	30	7.4
3, CC	307	Lower Pliocene	Light gray nanno ooze	37.9	37.5	0.36	2.36	1.44	1875	64.92	3.02	1.0	0.6	1895	110.1	110.0	27	7.2
4, CC	339	Lower Pliocene	Dark grayish brown marl ooze	39.2	38.6	0.35	2.48	1.36	1924	66.82	3.11	0.7	0.4	1948	113.4	113.8	22	7.3
Holes 125 & 125A (34° 37.49′N, 20° 25.76′E, water depth 2782m, Mediterranean Ridge in the Ionian Basin)																		
Surface ocean water				12.0	11.7	0.42	0.47	1.40	660	21.52	3.10	3.3	0.20	674	39.1	39.0	–	–
125-3-5	23	Quaternary	Brownish and greenish gray nanno ooze with foram and sapropel beds	12.1	11.6	0.49	0.55	1.34	656	21.85	2.85	2.4	0.15	671	39.3	39.0	27	7.4
5-1	41	Upper Pliocene	Brown to yellowish brown nanno ooze, deformed	12.3	12.0	0.51	0.62	1.35	676	22.44	2.76	2.6	0.16	692	40.1	41.2	22	7.5
125A-3-CC	53	Upper Pliocene	Light gray nanno ooze with forams	12.8	12.1	0.51	0.69	1.39	688	22.93	3.33	1.9	0.11	718	41.8	40.7	31	7.7
125-7-4	59	Upper Pliocene	Light yellowish brown nanno ooze, disturbed by drilling	12.2	12.1	0.49	0.60	1.39	683	22.25	2.97	2.6	0.16	691	40.1	40.7	–	7.7

TABLE 1 – *Continued*

Holes 125 and 125A (Continued)																		
125A-6-CC	80	Lower Pliocene	Olive green nanno ooze	13.2	12.5	0.57	0.98	1.47	728	23.84	3.65	2.9	0.18	758	43.9	44.6	29	7.9
9-CC	102	Upper Miocene	Dark gray dolomite, plastic	14.8	14.7	0.70	1.49	1.91	886	27.47	5.69	2.0	0.12	895	52.2	52.8	–	7.6
Hole 126 (35° 09.72'N, 21°, 25.63'E, water depth 3730m, Mediterranean Ridge Cleft in the Ionian Basin)																		
126-1-6	41	Quaternary	Olive gray marl ooze homogenous, plastic	12.0	11.6	0.37	0.26	1.12	619	21.71	1.15	–	–	636	36.6	36.8	28	7.7
2-4	79	Quaternary	Gray and brown nanno ooze and marl ooze	12.3	12.1	0.33	0.36	1.08	640	22.70	0.36	4.0	0.24	651	37.4	37.4	32	7.5
Holes 127 & 127A (35° 43.90'N, 22° 29.81'E, water depth 4654m, Northeast Margin, Hellenic Trench)																		
Surface ocean water				12.1	11.9	0.42	0.48	1.42	667	21.66	3.25	2.7	0.16	680	39.5	39.3	–	–
127-1-3	22	Quaternary	Gray and olive gray nanno to marl ooze with sand, disturbed by drilling	12.4	11.5	0.37	0.33	1.25	630	21.59	2.64	5.3	0.32	668	38.9	38.0	33	7.6
3-5	42	Quaternary	Olive gray marl ooze disturbed by drilling	12.5	12.1	0.37	0.23	1.08	635	22.27	0.87	6.1	0.37	652	37.7	37.4	–	7.7
127A-3-4	50	Quaternary	Dark gray to olive gray marl ooze, homogeneous	13.3	12.8	0.36	0.20	1.04	663	24.00	<0.05	7.5	0.46	684	39.4	39.0	33	7.7
4-4	77	Quaternary	Gray and dark gray marl ooze, plastic, gassy	16.6	16.2	0.42	0.35	1.20	832	30.00	<0.05	2.0	0.12	848	48.7	48.4	–	7.7
127-4-2	91	Quaternary	Dark greenish gray marl ooze, graded sand and silt	16.0	15.6	0.40	0.35	1.21	804	29.22	<0.05	1.9	0.12	825	47.3	47.8	29	7.6
6-5	108	Quaternary	Dark greenish gray marl ooze, plastic	19.7	19.5	0.45	0.55	1.52	1012	36.08	<0.05	3.5	0.21	1021	58.5	58.8	–	7.2
8-4	172	Quaternary	Olive gray nanno ooze with olive black sand layer below	37.9	34.4	0.55	1.00	1.33	1670	64.41	0.18	1.1	0.06	1821	105.4	104.5	27	7.3
9, CC	233	Quaternary	Varicolored gray silt to clay, nannos abundant	42.5	42.1	0.71	3.29	2.26	2199	76.81	2.40	0.7	0.04	2217	128.0	130.9	–	7.2
10, CC	284	Quaternary	Olive gray nanno ooze	44.1	44.9	0.80	3.62	2.33	2345	82.08	3.09	1.2	0.07	2380	136.1	140.8	24	7.0
11, CC	308	Quaternary	Light gray nanno ooze	43.7	41.2	0.73	3.17	2.27	2156	78.25	2.82	0.8	0.05	2266	131.0	132.6	27	7.2
12, CC	336	Quaternary	Olive gray nanno ooze, plastic to stiff	46.7	45.9	0.80	2.87	2.45	2362	82.91	2.79	0.7	0.04	2397	138.6	140.8	23	7.3
15, CC	427	Quaternary	Olive gray nanno ooze, plastic to stiff	52.4	50.9	0.79	2.17	2.01	2510	89.42	2.51	1.1	0.07	2575	149.4	150.7	–	7.5
Hole 128 (35° 42.58'N, 22° 28.10'E, water depth 4640m, SW margin Hellenic Trench)																		
128-2-4	56	Quaternary	Olive gray marl ooze, gassy	15.5	15.2	0.45	0.32	1.41	805	28.72	<0.05	4.8	0.29	820	46.9	48.4	28	7.6
5-6	153	Quaternary	Olive gray nanno ooze with graded layers of sand, gassy	26.0	25.3	0.55	1.65	3.68	1499	54.32	<0.05	1.1	0.06	1533	86.3	90.8	24	7.6
7-6	252	Quaternary	Olive gray nanno ooze, plastic to stiff, gassy	38.1	36.8	0.73	1.55	3.68	1999	72.98	<0.05	0.6	0.04	2059	117.1	121.6	23	7.8
8, CC	313	Quaternary	Olive gray and dark greenish gray marl ooze	43.2	42.3	0.59	1.36	3.17	2186	78.79	<0.05	0.9	0.06	2223	127.2	132.0	23	7.3

TABLE 1 – *Continued*

Sample Designation	Depth (m)	Age	Description	Na[a]	Na[b]	K	Ca	Mg	Total Cations (meq/kg)	Cl	SO_4	Alk. (meq/kg)	HCO_3[c]	Total Anions (meq/kg)	Sum[d]	Refractometer	H_2O[e] (‰)	pH
Hole 130 (33° 36.31′N, 27° 51.99′E, water depth 2979, Mediterranean Ridge in the Levantine Basin)																		
130-1-3	31	Quaternary	Light gray to olive gray nanno ooze, odor of H_2S	11.8	11.3	0.41	0.32	0.93	595	21.18	0.51	7.1	0.43	614	35.6	35.8	35	7.8
6, CC	418	Quaternary	Dark gray clay and greenish gray nanno ooze, sharp contact between Nile clay and pelagic deposits	13.2	13.1	0.31	0.50	1.00	683	24.41	0.08	0.6	0.04	690	39.5	40.2	31	7.9
Hole 132 (40° 15.70′ N, 11° 26.47′E, water depth 2835m, Tyrrhenian Basin)																		
132-2-3	16	Quaternary	Light olive gray nanno ooze	11.7	11.6	0.43	0.54	1.37	654	21.29	2.76	2.7	0.16	660	38.3	39.0	47	7.4
4-5	33	Quaternary	Yellow brown nanno ooze	11.6	11.4	0.39	0.60	1.40	651	21.36	2.56	3.0	0.18	658	38.1	38.5	40	7.3
6-3	48	Quaternary	Light olive gray nanno ooze, moderately deformed	11.7	11.5	0.35	0.68	1.42	660	21.42	3.03	3.1	0.19	670	38.8	39.6	33	7.2
8-4	68	Quaternary	Olive gray nanno ooze, deformed	11.9	11.6	0.35	0.79	1.44	670	21.81	3.31	2.3	0.14	686	39.7	40.2	35	7.2
10-5	87	Upper Pliocene	Brown foram-nanno ooze	–	11.7	0.35	(1.24)[f]	1.48	–	22.16	3.52	2.0	0.12	700	40.4	41.8	31	7.2
12-5	105	Upper Pliocene	Light olive gray foram-nanno ooze	12.0	12.0	0.34	1.10	1.52	712	22.44	3.79	2.1	0.13	713	41.3	42.4	32	7.2
15-4	130	Lower Pliocene	Pale yellow foram-nanno ooze	12.8	12.5	0.34	1.37	1.58	750	23.86	4.21	1.7	0.11	762	44.3	45.6	29	7.4
17-4	148	Lower Pliocene	Light olive gray nanno ooze	12.1	13.5	0.37	1.64	1.75	820	23.62	4.53	1.0	0.06	761	44.1	45.6	29	7.0
19-3	168	Lower Pliocene	Light olive gray nanno ooze	12.4	12.3	0.32	1.60	1.64	758	23.64	4.65	1.1	0.07	764	44.3	46.2	29	6.8

[a]Sodium determined by difference between anions and cations excluding Na.

[b]Sodium determined directly.

[c]HCO_3 is calculated from total alkalinity, assuming this is entirely due to bicarbonate ion.

[d]The sum incorporates the calculated Na values. Minor constituents are not included, but with the exception of strontium in some samples contribute less than 0.1 ‰ to the sum.

[e]pH and water content are taken from shipboard summaries.

[f]Value determined by difference.

TABLE 2
Minor Constituents of Pore Fluids. Concentrations in mg/kg (ppm)

Sample Designation	Depth (m)	Age	Description	B	Sr	Ba	Si(col.)[a]	Si(spec.)[b]
Hole 121								
Surface ocean water				5	8	<0.3	3.6	5
121-1-3	65	Quaternary	Dark greenish gray marl ooze, plastic	4	10	15	13	12
3-3	160	Quaternary	Dark greenish gray marl ooze, plastic	4	24	42	17	19
4-4	252	Quaternary	Dark greenish gray marl ooze, plastic to stiff	–	–	–	7.3	–
Hole 122								
122-2-2	95	Upper Pliocene	Varicolored brown and gray alternations of fine sands and clays	7	30	0.4	4.3	9
Hole 123								
123-1-3	85	Quaternary	Olive gray clays and sand, turbidites	4	23	<0.3	10	6
5-2	219	Lower Pliocene	Varicolored gray and brown nanno to marl ooze, fine layers of silt or fine sand	9	58	<0.3	5.8	8
Hole 124								
124-1, CC	128	Pleistocene	Varicolored gray terrigenous nanno ooze, plastic, mottling	4	58	< 0.3	4.7	6
3, CC	307	Lower Pliocene	Light gray nanno ooze	9	106	0.3	<2	4
4, CC	339	Lower Pliocene	Dark grayish brown marl ooze	8	101	< 0.3	–	4
Holes 125 and 125A								
Surface ocean water				5	9	<0.3	<2	<2
125-3-5	23	Quaternary	Brownish and greenish gray nanno ooze with foram and sapropel beds	5	17	<0.3	4.4	6
5-1	41	Upper Pliocene	Brown to yellowish brown nanno ooze, deformed	8	19	<0.3	3.0	5
125A-3, CC	53	Upper Pliocene	Light gray nanno ooze with forams	5	21	<0.3	4.6	5
125-7-4	59	Upper Pliocene	Light yellowish brown nanno ooze, disturbed by drilling	9	19	<0.3	9.8	10
125A-6, CC	80	Early Pliocene	Olive green nanno ooze	6	30	<0.3	4.8	5
9, CC	102	Upper Miocene	Dark gray dolomite, plastic	9	37	<0.3	20	18
Hole 126								
126-1-6	41	Quaternary	Olive gray marl ooze homogeneous, plastic	6	15	<0.3	–	6
2-4	79	Quaternary	Gray and brown nanno ooze and marl ooze	5	20	0.3	6.4	8
Holes 127 and 127A								
Surface ocean water				5	9	<0.3	<2	<2
127-1-3	22	Quaternary	Gray and olive gray nanno to marl ooze with sand, disturbed by drilling	5	10	<0.3	7.0	7
3-5	42	Quaternary	Olive gray marl ooze disturbed by drilling	8	10	0.6	3.4	7
127A-3-4	50	Quaternary	Dark gray to olive gray marl ooze, homogeneous	5	11	18	9.3	9
4-4	77	Quaternary	Gray and dark gray marl ooze, plastic, gassy	4	20	30	8.1	7
127-4-2	91	Quaternary	Dark greenish gray marl ooze, graded sand and silt	6	19	2.4	7.3	8
6-5	108	Quaternary	Dark greenish gray marl ooze, plastic	5	26	52	14.4	16
8-4	172	Quaternary	Olive gray nanno ooze with olive black sand layer below	5	89	7	4.5	14
9, CC	233	Quaternary	Varicolored gray silt to clay, nannos abundant	12	158	0.4	4.9	7
10, CC	284	Quaternary	Olive gray nanno ooze	29	164	0.3	2.0	4
11, CC	308	Quaternary	Light gray nanno ooze	21	149	<0.3	2.4	5
12, CC	336	Quaternary	Olive gray nanno ooze, plastic to stiff	22	180	<0.3	3.1	5
15, CC	427	Quaternary	Olive gray nanno ooze, plastic to stiff	23	137	<0.3	<2	9
Hole 128								
128-2-4	56	Quaternary	Olive gray marl ooze, gassy	6	20	63	5.1	6
5-6	153	Quaternary	Olive gray nanno ooze, with graded layers of sand, gassy	5	240	214	<2	6
7-6	252	Quaternary	Olive gray nanno ooze, plastic to stiff, gassy	3	345	216	<2	4
8, CC	313	Quaternary	Olive gray and dark greenish gray marl ooze	2	275	216	7.9	12

TABLE 2 – *Continued*

Sample Designation	Depth (m)	Age	Description	B	Sr	Ba	Si (col)[a]	Si (spec.)[b]
Hole 130								
130-1-3	21	Quaternary	Light gray to olive gray nanno ooze, odor of H_2S	4	15	0.6	8.5	9
6, CC	418	Quaternary	Dark gray clay and greenish gray nanno ooze, sharp contact between Nile clay and pelagic deposits	2	24	2.3	3.9	7
Hole 132								
132-2-3	16	Quaternary	Light olive gray nanno ooze	7	16	<0.3	10	9
4-5	33	Quaternary	Yellow brown nanno ooze	8	22	<0.3	4.3	5
6-3	48	Quaternary	Light olive gray nanno ooze, moderately deformed	7	23	<0.3	13	10
8-4	68	Quaternary	Olive gray nanno ooze, deformed	6	30	<0.3	7.2	8
10-5	87	Upper Pliocene	Brown foram-nanno ooze	7	35	<0.3	4.5	7
12-5	105	Upper Pliocene	Light olive gray foram-nanno ooze	8	37	<0.3	5.3	7
15-4	130	Lower Pliocene	Pale yellow foram-nanno ooze	8	41	<0.3	4.7	6
17-4	148	Lower Pliocene	Light olive gray nanno ooze	7	41	<0.3	<2	6
19-4	168	Lower Pliocene	Light olive gray nanno ooze	8	47	<0.3	5.7	6

[a](col.) = Colorimetric determination

[b](spec.) = Emission spectographic determination.

tions are altered 5 per cent or less (Sayles *et al.*, 1972). K concentrations may be significantly affected. Gains of up to .08 g/kg have been observed (Bischoff *et al.*, 1970; Sayles *et al.*, 1972).

Enrichments of Na and Cl are found at all of the sites sampled for interstitial water studies. At Sites 122, Valencia Trough, and 126, Mediterranean Ridge, the Cl increases are small but above analytical uncertainty. Evaporation prior to squeezing or inadequate sealing of storage vessels could have produced these small increases, but the increase in Cl with depth at Site 126 suggests the conclusion that real Cl gradients exist at least at this site. The increases in Na and Cl found at all of the other sites sampled on Leg 13 are large enough to avoid uncertainty as to the existence of *in situ* enrichments. Where sufficient samples exist, these increases can be seen to be roughly linear as a function of depth. Cl concentrations of 25 to 30 g/kg are common with maximum values of 89 and 79 g/kg occurring at Sites 127 and 128, respectively.

At Sites 122 and 124 in the western Mediterranean, 125 and 127 in the eastern Mediterranean, and 132 in the Tyrrhenian Sea, the influence of underlying evaporites appears to exert a dominant influence on SO_4 concentrations and in some instances on Mg (124, 127, 132). Ca concentrations appear to reflect the interaction of both diagenetic and evaporitic influences. Gypsum or anhydrite was recovered in cores from each of these sites except 127 where penetration was terminated before reaching the level of the evaporite formation. Not surprisingly, the pore waters commonly are characterized by Ca and SO_4 enrichments. Relative to standard seawater (Ca = 0.41 g/kg, SO_4 = 2.71 g/kg), nine-fold Ca increases (to 3.62 g/kg) and two-fold SO_4 enrichments (to 5.69 g/kg) are found. Mg concentrations in excess of seawater (1.29 g/kg) are observed at Sites 124 (slight), 125, 127 and 132, reaching concentrations of 2.45 g/kg at Site 127 with values exceeding 1.5 g/kg common.

At Sites 121 (Alboran Basin), 123 (Valencia Trough), and 126 and 130 on the Mediterranean Ridge, Ca, Mg and SO_4 concentrations chiefly reflect the influence of diagenetic reactions rather than that of evaporites at depth. In the absence of evaporites, Mg concentrations have been found to invariably decrease with depth. Depletions of Mg may be related to dolomitization (Sayles *et al.*, 1972; Broecker, 1972) or to silicate reactions such as those proposed by Drever (1971). Mg depletions are found in Quaternary sediments at Sites 121, 126, 130 and the upper portion of 127. The depletions of Mg (to 0.9 - 1.1 g/kg) are compatible with earlier DSDP pore water data. Depletions of SO_4 are also a common product of diagenesis and result from bacterial reduction of SO_4. Depletion of more than 80 per cent of the original SO_4 present is found at Sites 121, 126 and 130. Smaller losses are found at Site 123. Ca depletion commonly accompanies strong SO_4 reduction at least in the upper portions of such sites (Gieskes, 1972; Sayles, *et al.*, 1972). Losses of Ca are found at Sites 121, 126 and 130, those sites marked by SO_4 depletion. With the possible exception of Sample 130-1-3, we believe the Ca losses are too large to be explained as an artifact resulting from the precipitation of $CaCO_3$ after squeezing. Once SO_4 reduction is virtually complete, further Ca depletion does not occur. At depth in these sites, depletion actually gives way to gradual Ca enrichment. This effect can be seen in the lowermost samples of Sites 121, 126 and 130. At sites where no appreciable SO_4 reduction occurs, Ca enrichment commonly is seen over the entire hole (cf. data Legs 8 and 15). Thus, all of the Ca, Mg and SO_4 changes occurring at Sites 121, 123, 126 and 130 can be adequately explained within the framework of diagenetic alterations noted in previous interstitial water studies.

Site 128 in the Hellenic Trench exhibits behavior characteristic of both evaporite influence and diagenesis. Concentrations of SO_4 are below our detection limit (.05 g/kg) in all samples from this site, reflecting complete

utilization in diagenetic reduction. The observed Ca enrichments (below 56 m) may reflect either diagenetic or evaporitic influence. Mg is strongly enriched reaching concentrations of 3.26 g/kg, the highest value recorded on Leg 13. As noted above, such enrichment has only been found where evidence of underlying evaporites exists. Site 127, located a few kilometers from Site 128, also exhibits a somewhat split personality. In the upper portions of this site (< 177 m) diagenetic reactions hold sway, but below this the influence of evaporites on Mg and SO_4 can be seen.

The concentrations of minor elements in the samples from Leg 13 exhibit some of the largest deviations from seawater found during the Deep Sea Drilling Project. Enrichments of Sr reached 180 ppm and 345 ppm in samples from Sites 127 and 128, respectively. Modest enrichments of 20 to 60 ppm are found in all of the other sites for which samples are available. Such modest enrichments are quite common in interstitial solutions of calcareous sediments from the Pacific Ocean and have been discussed in earlier leg reports (e.g. Legs 7 and 8). Ba concentrations markedly higher than any reported previously by us are found at Site 128 (up to 216 ppm), and unusually high values are found at Sites 121 and 127. As has been noted previously, Ba enrichments are characteristic of sites exhibiting extensive SO_4 reduction, indicating that barite solubility is the primary control of concentration. The extremely high values at Site 128 may well represent other unidentified influences, however. The reduction of SO_4 to our detection limit is common, but concentrations even approaching those at 128 have not been seen previously. The unusually high Mg and Sr also suggest abnormal conditions at this site. While the B data exhibit considerable scatter, real enrichment relative to seawater is usually found at the Leg 13 sites where evaporites appear to influence Mg or SO_4. Concentrations commonly fall in the range 6 to 9 ppm at these sites. At 127, B is strongly enriched to 20 to 29 ppm in the lower portion of the hole.

DISCUSSION

The existence of Na and Cl gradients at all but two sites for which interstitial water sampling was carried out indicate that halite or brine-containing evaporites exist at depth at all of these sites. The two remaining sites (122 and 126) exhibit small chloride enrichments, but sampling was too sparse and shallow to definitely prove the existence of Na and Cl enrichments and gradients characteristic of sediments overlying salt deposits. Although halite was not recovered at any of the above sites, we believe that Na and Cl data provide sufficient evidence for concluding that such sediments do exist at depth at all of the sites except perhaps 122 and 126.[1] This conclusion is in agreement with seismic data which also suggest that a halite layer exists below the deepest penetration at these sites.

Site 121 was terminated in a schist which, in the preliminary report, is presumed to be basement. The interstitial waters of Site 121 are characterized by Na and Cl gradients typical of sediments overlying salt. This site was drilled over a basement high onto which Pliocene and Miocene sediments lap unconformably (W. B. F. Ryan, personal communication). Thus, some lateral movement of brines from the Miocene or Pliocene sediments must occur to account for the observed gradients. There is little question that halite or brine-containing sediments do exist near this site.

Enrichments of SO_4 have not been found previously in interstitial waters sampled by the DSDP. There is little doubt that the enhanced SO_4 concentrations, common in these pore fluids, result from the dissolution of gypsum or anhydrite. With one exception, the SO_4 enrichments are found at sites where evaporitic gypsum or anhydrite was recovered (Sites 122, 124, 125, 132). Site 132 appears to provide the most straightforward example of the influence of anhydrite dissolution upon overlying sediments. As seen in Figure 1, ΔCa and ΔSO_4 (Δ = change in pore water concentration relative to seawater) vary linearly suggesting that dissolution and diffusion are responsible for the observed concentration increases. The slope of the ΔCa-ΔSO_4 correspondence is not 1 as required by simple dissolution, but rather 1.5. Consequently, some concurrent reaction must either supply Ca or remove a fraction of the SO_4 released by dissolution. Both reactions have been frequently observed in previous DSDP studies. At the other sites where evaporitic sediments were cored, no simple and consistent relationship between Ca and SO_4 can be determined. Insufficient data are available at Sites 122 and 124, and the data of 125 exhibit no consistent trend.

In several earlier legs of the DSDP (e.g., 7, 8, and 15) a nearly linear correspondence between Ca and Sr enrichment was found to exist. A similar correspondence appears to hold for all of the Leg 13 sites where sufficient data are available for interpretation. At least at Site 132 the linear variations of ΔCa, ΔSO_4 and ΔSr indicate that the Sr is

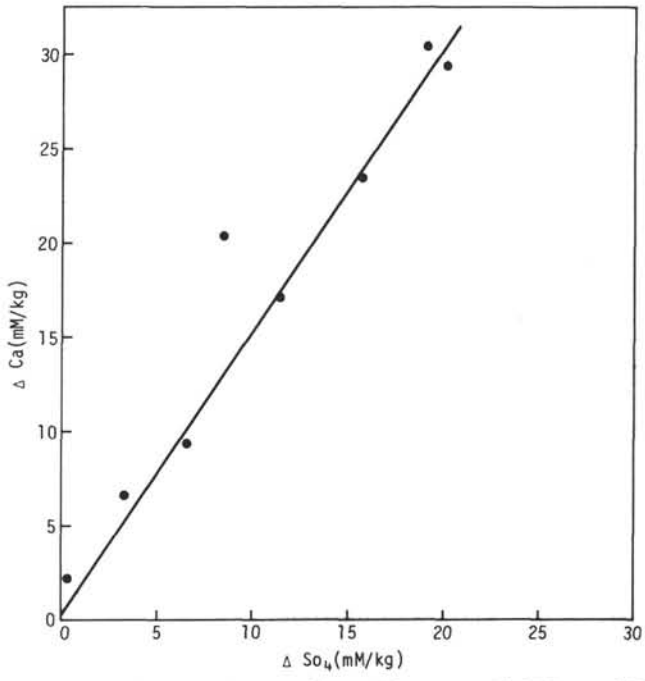

Figure 1. *The variation in Ca enrichment with SO_4 enrichment (Δ = pore water concentration – standard seawater concentration.) Data are for Site 132 only.*

released during dissolution and possibly recrystallization of gypsum and anhydrite. The slopes of the data plots in Figure 2 are in the range 60 to 70. This requires that between 1 and 2 per cent of the Ca ion sites in a presumed $CaSO_4$ phase be occupied by Sr if solution of $CaSO_4$ is responsible for the observed enrichments. Since most marine gypsum and anhydrite rocks contain < 0.2 per cent Sr (Stewart, 1963; F. T. Manheim, unpublished data), we presume that much of the Sr is released during recrystallization.

The abnormally high concentrations of Mg observed at Sites 127, 128 and 132 are difficult to explain. Normal diagenetic changes lead to the depletion of Mg, whereas the increases noted above are believed due to the influence of evaporitic sediments. Late stage evaporites, in particular, contain readily soluble Mg-bearing minerals and could supply Mg. The data argue against any simple explanation, however, for at least Sites 127 and 128, Mg concentrations pass through a maximum. This is also true of Mg at 132, but the drop in the lowermost sample is small and a maximum is not well established. Maxima in Mg *vs.* depth

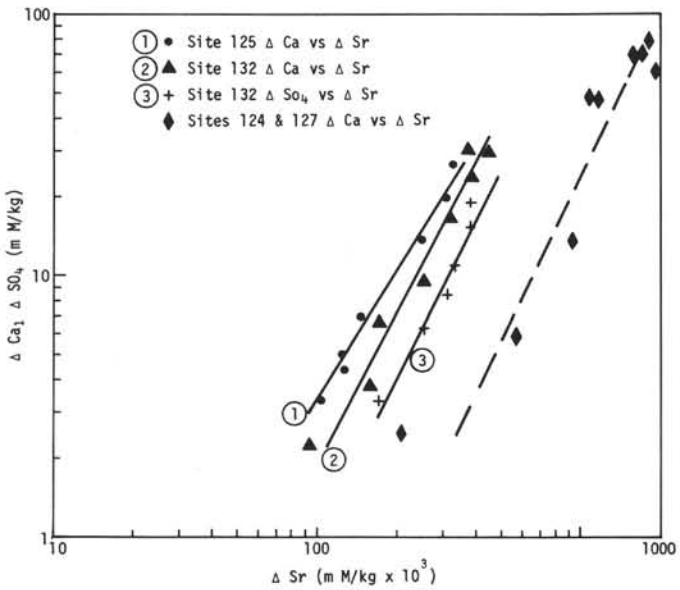

Figure 2. *The variation of Sr enrichment with Ca and SO_4 enrichment for Site 132 and Ca enrichment only for Sites 124, 125 and 127. (Δ = pore water concentration – standard seawater concentration).*

profiles have also been found associated with known or inferred evaporites in the Gulf of Mexico by Manheim and Bischoff (1969) in core 26 and at DSDP Site 92 (Leg 10). Such maxima cannot be explained by diffusive fluxes of Mg from late stage evaporites at depth, and diagenetic reactions must be responsible. This type of Mg *vs.* depth distribution is associated with evaporitic sediments, but we do not know the nature of the reactions occurring.

REFERENCES

Bischoff, J. L., Greer, R. E. and Luistros, A. O., 1970. Composition of interstitial waters of marine sediments: temperature of squeezing effect. *Science.* **167**, 1245.

Broecker, W. S., 1972. Initial Reports of the Deep Sea Drilling Project, Volume 15 (in press).

Drever, J. I., 1971. Magnesium-iron replacement in clay minerals in anoxic marine sediments. *Science.* **172**, 1334.

Fanning, D. K. and Pilson, M. E. Q., 1971. Interstitial silica and pH in marine sediments: some effects of sampling procedure. *Science.* **173**, 1228.

Gieskes, J. M. Interstitial water studies, Leg 15. **In** Edgar, N. T. and Saunders, J. B., *et al.*, 1972. Initial Reports of the Deep Sea Drilling Project, Volume 15. Washington (U.S. Government Printing Office) (in preparation).

Mangelsdorf, P. C., Jr., Wilson, T. R. S. and Daniell, E., 1969. Potassium enrichments in interstitial waters of marine sediments. *Science.* **165**, 171.

Manheim, F. T. and Bischoff, J. L., 1969. Geochemistry of pore waters from Shell Oil Company drill holes on the continental slope of the northern Gulf of Mexico. *Chem. Geol.* **4**, 63.

Manheim, F. T. and Sayles, F. L., 1969. Interstitial Water studies on small core samples, Deep Sea Drilling Project, Leg 1. **In** Ewing, M. and Worzel, J. L., *et al.*, 1969. *Initial Reports of the Deep Sea Drilling Project, Volume 1.* Washington (U.S. Government Printing Office), 403.

Manheim, F. T., Sayles, F. L. and Waterman, L. S. Interstitial water studies on small core samples, Leg 10. **In** Worzel, J. L. and Bryant, W. R., *et al., Initial Reports of the Deep Sea Drilling Project, Volume 10.* Washington, D. C. (U.S. Government Printing Office) (in preparation).

Sayles, F. L., Manheim, F. T. and Waterman, L. S. Interstitial water studies on small core samples, Leg 15. **In** Edgar, N. T. and Saunders, J. B., *et al., Initial Reports of the Deep Sea Drilling Project, Volume 15.* Washington, D.C. (U.S. Government Printing Office) (in preparation).

Stewart, F. H., 1963. Marine Evaporites. U.S. Geol. Surv. Prof. Paper, 440-y.